Validity of the continuum approach to optical phonons in short-period superlattices

1990 J. Phys.: Condens. Matter 2 4363

(http://iopscience.iop.org/0953-8984/2/19/005)

J. Phys.: Condens. Matter **2** (1990) 4363–4369. Printed in the UK

Validity of the continuum approach to optical phonons in short-period superlattices

F Bechstedt and H Gerecke
Friedrich-Schiller-Universität, Max-Wien-Platz 1, DDR-6900 Jena, German Democratic Republic

Received 10 October 1989, in final form 18 January 1990

Abstract. We report a strict comparison of long-wavelength optical lattice vibrations in a superlattice obtained within the macroscopic continuum model and a closely parallel microscopic model. It is shown that the proper envelopes of the atomic displacement patterns can be found if the uncertainties inherent in any dispersionless theory such as the continuum model are appropriately treated. Apart from small discrepancies due to the discrete nature of the matter and effective material layer thicknesses the main failure of the continuum theory is the neglect of bulk phonon dispersion.

The interpretation of recent Raman scattering studies [1–4] of long-wavelength optical phonons in short-period superlattices, particularly $(GaAs)_{N_1}(AlAs)_{N_2}(001)$ superlattices, indicates discrepancies in the treatment of Fröhlich as well as deformation potential electron–phonon interactions in the framework of the conventional dielectric continuum theory [5–8]. For systems involving thin layers this theory seems to be beyond its legitimate limit. The atomic displacements do not fulfil the continuity condition at the interfaces. Microscopic descriptions [9–12] appear to be necessary.

For that reason, in this paper we present a critical comparison of the results for the atomic displacements obtained within the continuum theory neglecting bulk phonon dispersion and a microscopic model including this dispersion and the atomic structure of matter by definition. Thereby the elastic and electric forces acting on the atoms are likewise treated. More strictly speaking, for the purpose of comparison with the continuum approach in the microscopic theory the elastic forces are described by one nearest-neighbour central-force constant and the electric field is spatially averaged with respect to the Wigner–Seitz cell of the FCC structure underlying the superlattice materials. As a result of the strict comparison of the microscopic and macroscopic theories in the case of long-wavelength optical phonons we derive conditions for the validity of the continuum approach and its dependence on layer thicknesses, phonon propagation direction and mode type.

Prototypes for superlattices formed by lattice-matched zincblende semiconductors and grown in the [001] direction are short-period $(GaAs)_{N_1}(AlAs)_{N_2}$ superlattices. They represent tetragonal crystals with $2(N_1 + N_2)$ atoms per elementary cell. Thereby the atoms can be labelled by a triple $s = abc$. The number $a = 1(2)$ indicates that the considered atom is a cation (anion). The index b characterises the material layer, GaAs ($b = 1$) or AlAs ($b = 2$), and c indicates the number of molecular layers parallel to the

0953-8984/90/194363 + 07 $03.50

interfaces, i.e. $1 \leqslant c \leqslant N_1$ for GaAs and $N_1 + 1 \leqslant c \leqslant N_1 + N_2$ for AlAs. For wavevectors from the centre of the superlattice Brillouin zone the equations of motion of the sth atom in the superlattice elementary cell with the mass M_s and the effective ion charge e_s can be written in the form [12]

$$\sum_{\substack{s' \\ (\leqslant NN)}} \left\{ M_{s'}\omega_j^2(\theta)\delta_{ss'} - \left(f_{b'} + \frac{4\pi e_{b'}^2}{\Omega_0}\delta_{\alpha z}\right)[\delta_{ss'} - \tfrac{1}{2}(1 - \delta_{ss'})] \right\} \frac{1}{\sqrt{M_{s'}}} e_{s'j\alpha}(\theta)$$
$$= -e_s[E_{jy}(\theta)\delta_{\alpha y} + D_{jz}(\theta)\delta_{\alpha z}] \tag{1}$$

for the frequency $\omega_j(\theta)$ and the polarisation vector components $e_{j\alpha}(\theta)$ ($\alpha = x, y, z$) of a long-wavelength phonon from the branch j and propagating in a certain direction $\bar{e}_{\bar{q}} = \sin\theta\,\bar{e}_y + \cos\theta\,\bar{e}_z$, where θ is the angle between $\bar{e}_{\bar{q}}$ and the superlattice axis $\bar{e}_z$. The driving forces on the right-hand side are related (apart from a certain constant) to the y component $E_{jy}(\theta)$ of the spatially averaged electric field and the z component $D_{jz}(\theta)$ of the dielectric displacement field. They are defined by

$$\begin{pmatrix} E_{jy}(\theta) \\ D_{jz}(\theta) \end{pmatrix} = -\sin\theta \frac{4\pi}{\Omega_0}\frac{1}{N_1 + N_2} \sum_{s=1}^{2(N_1+N_2)} \frac{e_s}{\sqrt{M_s}} \begin{pmatrix} \sin\theta & \cos\theta \\ \cos\theta & -\sin\theta \end{pmatrix} \begin{pmatrix} e_{sjy}(\theta) \\ e_{sjz}(\theta) \end{pmatrix} \tag{2}$$

where the volume $\Omega_0 = a^3/4$ (where a is the bulk lattice constant) of the zincblende Wigner–Seitz cell is introduced and $e_{1b} = -e_{2b} = e_b$ is assumed because of the charge neutrality.

The short-range part of the effective dynamic matrix on the left-hand side of (1) is restricted to the interaction of the first-nearest-neighbour atomic planes parallel to the interfaces. It is angle independent. However, its electrical contribution affects only displacements parallel to the superlattice axis $\bar{e}_z$. The electric-field-induced forces on the right-hand side of (1) produce a strong asymmetry with θ in the lattice vibrations corresponding to the reduced symmetry of the superlattice. We mention that because of the independence of the long-range fields $E_{jy}(\theta)$ and $D_{jz}(\theta)$ (2) of atomic number s the conventional boundary conditions of electrostatics at interfaces are automatically fulfilled. In spite of the simplicity the equations of motion have to be solved numerically taking into account appropriate parameters for GaAs and AlAs [12].

The continuum theory is directly aimed at optical phonons. We therefore introduce the relative atomic displacement field for each molecule within a superlattice elementary cell by $\bar{e}_{bj}(c, \theta) = \sqrt{\mu_b/M_{1b}}\,\bar{e}_{1bj}(\theta) - \sqrt{\mu_b/M_{2b}}\,\bar{e}_{2bj}(\theta)$, where μ_b denotes the reduced mass of a molecule in the material layer $b = 1, 2$. The formal transition of the microscopic theory (1) to the continuum approach can be done taking the limit of vanishing atomic distances, i.e. $a \to 0$, under conservation of the material layer thicknesses $d_b = N_b a/2$. Introducing the continuous distance of molecules given by $z = ca/2$ ($a \to 0$) and neglecting the bulk phonon dispersion, one gets, for $0 < z < d_1 + d_2 = d$,

$$[\omega_j^2(\theta) - \omega_{\mathrm{TO}b}^2(\delta_{\alpha x} + \delta_{\alpha y}) - \omega_{\mathrm{LO}b}^2\delta_{\alpha z}]e_{bj\alpha}(z, \theta)$$
$$= -(e_b/\sqrt{\mu_b})[E_{jy}(\theta)\delta_{\alpha y} + D_{jz}(\theta)\delta_{\alpha z}] \tag{3}$$

with the bulk zone-centre phonons

$$\omega_{\mathrm{TO}b}^2 = f_b/\mu_b \qquad \omega_{\mathrm{LO}b}^2 = (f_b + 4\pi e_b^2/\Omega_0)/\mu_b \tag{4}$$

and the electric field components

$$\begin{pmatrix} E_{jy}(\theta) \\ D_{jz}(\theta) \end{pmatrix} = -\sin\theta \frac{4\pi}{\Omega_0} \sum_{b=1}^{2} \frac{e_b}{\sqrt{\mu_b}} \frac{1}{d} \int_{d_1\delta_{b2}}^{d_1\delta_{b2}+d_b} \mathrm{d}z \begin{pmatrix} \sin\theta & \cos\theta \\ \cos\theta & -\sin\theta \end{pmatrix} \begin{pmatrix} e_{bjy}(z, \theta) \\ e_{bjz}(z, \theta) \end{pmatrix} \tag{5}$$

which are related to each other by $\bar{D}_j(z, \theta) = \bar{E}_j(z, \theta) + (4\pi e_b/\Omega_0\sqrt{\mu_b})\bar{e}_{bj}(z, \theta)$.

The system of equations of motion (3) can be solved analytically. There are two types of solution. The first type of solution, the confined optical phonons with frequencies and polarisation directions according to

$$\omega_j(\theta) = \omega_{\mathrm{TO}b} \qquad \bar{e}_{bj}(z,\theta) \parallel \bar{e}_x \qquad j = \mathrm{TO}n \text{ (s polarised)}$$

$$\omega_j(\theta) = \omega_{\mathrm{TO}b} \qquad \bar{e}_{bj}(z,\theta) \parallel \bar{e}_y \qquad j = \mathrm{TO}n \text{ (p polarised)}$$

$$\omega_j(\theta) = \omega_{\mathrm{LO}b} \qquad \bar{e}_{bj}(z,\theta) \parallel \bar{e}_z \qquad j = \mathrm{LO}n \text{ (p polarised)}$$

for the GaAs-like ($b = 1$) and AlAs-like ($b = 2$) modes ($n = 1, 2, 3, \ldots$), are characterised by vanishing right-hand sides of equations (3), i.e. $E_{jy}(\theta) = D_{jz}(\theta) = 0$.

In the case of s-polarised TOn (arbitrary θ and n), antisymmetric p-polarised TOn/LOn (arbitrary θ, even n) and p-polarised TOn/LOn ($\theta = 0$, arbitrary n) vibrations the condition $E_{jy}(\theta) = D_{jz}(\theta) = 0$ is automatically fulfilled and does not give rise to any restrictions for the solutions. Because of the neglect of the dispersion of the bulk phonon branches, each vibronic level $\omega_j(\theta)$ is independent of the mode index n and, hence, highly degenerate. Each orthonormalised and complete set of functions defined in the interval $0 < z - d_1\delta_{b2} < d_b$ can be assumed. Starting from the idea of standing waves as in the conventional continuum theory [5–8] and in agreement with results of the microscopic theory (1) we compose the solutions of trigonometric functions and constants (cf equation (6)). Additionally we assume continuity of the relative atomic displacements [13, 14]. This boundary condition corresponds to the vanishing of the displacements at the interfaces contrary to the solution for confined phonons usually quoted in the literature [5, 7]. The confinement gives rise to wavevectors $q_n^b(\theta) = \pi n/d_b$ for these modes. In the case of symmetric p-polarised TOn/LOn modes ($\theta > 0$, odd n) the zero-field components $E_{jy}(\theta) = D_{jz}(\theta) = 0$ correspond to an additional condition. Treating again the arbitrariness of the solutions in a suitable way the resulting orthonormalised set of envelope functions can be written as ($0 < z - d_1\delta_{b2} < d_b$)

$$e_{bj\alpha}(z,\theta) = \sqrt{2/d_b}\begin{cases} \{\cos[q_n^b(\theta)(z - d_1\delta_{b2} - d_b/2)] \\ \qquad - \cos[q_n^b(\theta)d_b/2]\}/\sin[q_n^b(\theta)d_b/2] & n = 1,3,5,\ldots \\ \sin[(\pi n/d_b)(z - d_1\delta_{b2} - d_b/2)] & n = 2,4,6,\ldots \end{cases} \tag{6}$$

where the confinement wavevector $q_n^b(\theta)$ satisfies the transcendental equation

$$q_n^b(\theta)d_b/2 = \tan[q_n^b(\theta)d_b/2] \tag{7}$$

for symmetric p-polarised TOn/LOn phonons and propagation directions $\theta > 0$. For all other superlattice phonon branches, $q_n^b(\theta) = \pi n/d_b$ holds in equation (6). We mention that there is no arbitrariness if bulk dispersion is included. In this case the boundary conditions for the electric fields as well as displacement fields can be simultaneously fulfilled. Then equation (6) can be obtained as an exact result in the limit of vanishing dispersion.

For $\theta > 0$ and $E_{jy}(\theta) \neq 0$, $D_{jz}(\theta) \neq 0$ there are no uncertainties, even in the dispersionless limit. The four p-polarised solutions of the system of integral equations (3) missing in the GaAs-like and AlAs-like systems of eigenvectors (6) and making these complete [7] are the well known macroscopic interface phonons of the Fuchs–Kliewer type [5, 7, 8]. The polarisation vectors $\bar{e}_{bj}(z, \theta)$ have properties which differ remarkably from those found for confined phonons [14].

(i) They are different from zero in GaAs as well as AlAs.

(ii) Their amplitude is constant with respect to z in each material layer.

(iii) Their direction varies between $\bar{e}_y$ and $\bar{e}_z$ depending on the propagation direction θ and the branch character j.

Contrary to the confined phonons the interface modes exhibit an angular dispersion according to the well known implicit dispersion relation [5, 7, 8] for the frequencies $\omega_j(\theta)$.

In the case of the p-polarised LOn phonons and $\theta > 0$ the same results have been derived by Huang and Zhu [13] for the macroscopic electrostatic potential $\Phi_{bj}(z, \theta)$. This can be verified by comparison of equation (6) in this work and equations (40) and (42) in [13] by means of the relation $\partial\Phi_{bj}(z, \theta)/\partial z \sim e_{bjz}(z, \theta)$. However, the integral equation formalism (3) for the relative atomic displacements is more general as the Laplace equation for the electrostatic potential. Applying the system of equations (3), information about the displacement fields can be also extracted in the limit of vanishing macroscopic electric fields, i.e. for s- and p-polarised TOn phonons. Apart from the generalisation of the results (6) for the TOn phonons the inclusion of the anisotropy between $\theta = 0$ and $\theta > 0$ is essential. It guarantees firstly the correct transition from a dispersionless theory to any theory considering the dispersion of bulk phonon bands and secondly a correct mode ordering as well as mode identification in agreement with the microscopic theory. For example, the second mode in figure 3 of [13] labelled $n = 3$, has to be identified with the dispersive microscopic LO1 mode for propagation parallel to the superlattice axis ($\theta = 0$) [14]. Its confinement wavevector $q_n^b(\theta) \simeq 2.9\pi/d_b$ for $\theta > 0$ cannot be related to the labelling $n = 3$. Rather it only indicates that the microscopic LO1 mode is for $\theta > 0$ lower in energy than for the microscopic LO2 mode.

The strict comparison of results from the microscopic and macroscopic theories requires some agreement and a mutual identification of the modes appearing in the two different approaches. More from a technical point of view we identify the positions of the interfaces $z = 0$, d_1, $d_1 + d_2$ in the continuum theory with those of the As layers between Ga and Al in the microscopic treatment. Comparing the envelopes (6) derived for relative displacements with cation or anion displacement patterns $\bar{e}_{sj}(\theta)$ resulting from (1) the normalisation has to be changed by a factor $(M_{ab}/\mu_b)^{1/2}$. The mode identification is somewhat problematical, especially for the p-polarised modes and propagation directions $\theta > 0$. For all other microscopic or macroscopic optical phonons the integer n corresponds to the number of nodes in the displacement pattern. Furthermore, the n sequence is directly related to the energy ordering, at least in the microscopic approach. In the case of p-polarised modes the energy arrangement of LOn or TOn can be destroyed for $\theta > 0$ owing to the angular dispersion of the superlattice [10, 12]. One question within the continuum theory concerns the assignment of one AlAs-like and GaAs-like LOn or TOn phonon to an interface mode. If an 'infinite small' bulk phonon dispersion and the limitation $n < N_b$ of the modes are taken into account one finds that for odd (even) N_b LON_b (LO($N_b - 1$)) and TO1 should be interface phonons [14].

One example for such a strict comparison of results from the macroscopic continuum theory and a parallel microscopic force constant model is given in figure 1. There the anion displacement patterns $\bar{e}_{sj}(\theta)$ of the symmetric p-polarised GaAs-like LOn and TOn modes are compared with the corresponding envelopes $\bar{e}_{bj}(z, \theta)$ (6) for phonon propagation parallel ($\theta = 0$) and perpendicular ($\theta = \pi/2$) to the superlattice growth direction. The modes are arranged according to the energy ordering—LO1, LO3, TO1, TO3, LO5, TO5, LO7 and TO7—resulting from the microscopic theory for $\theta = 0$. Generally

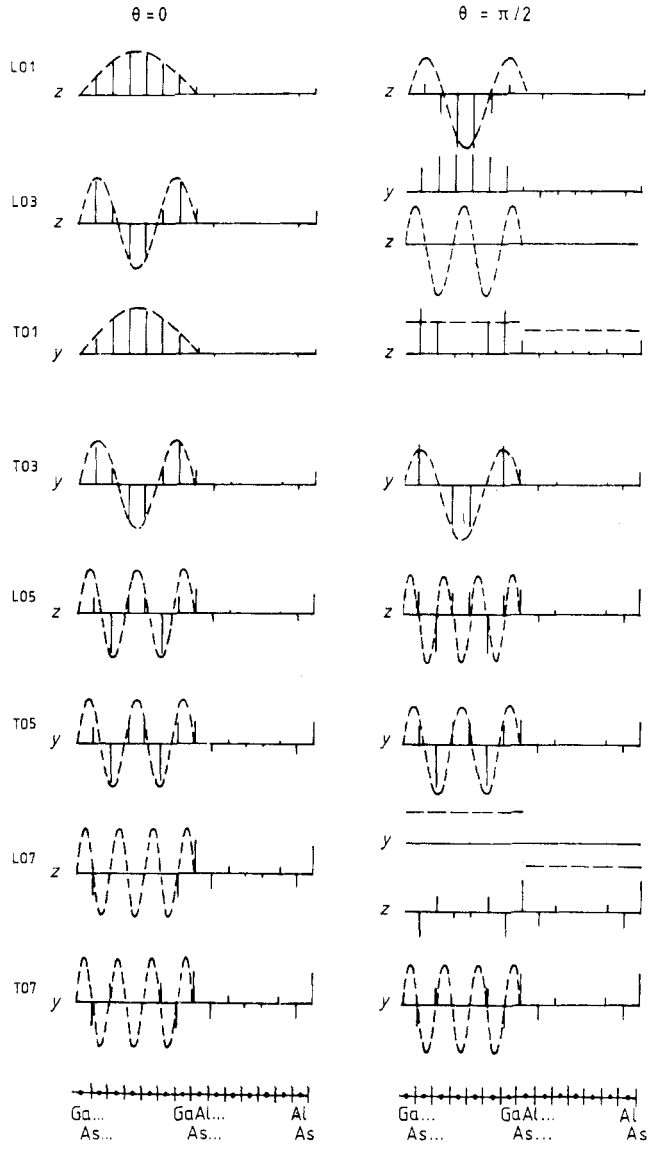

Figure 1. Anion displacement patterns of the GaAs-like p-polarised symmetric long-wavelength LOn and TOn modes of a $(GaAs)_7(AlAs)_7$ (001) superlattice shown as vertical lines for phonon propagation parallel ($\theta = 0$) and perpendicular ($\theta = \pi/2$) to the growth direction. The envelope functions (6) resulting within the dispersionless continuum theory are shown for comparison (– – –).

the polarisation direction $z(y)$ for the confined LOn (TOn) phonons is presented. In the $\theta = \pi/2$ case both polarisation directions y and z are drawn if the microscopic theory and continuum approach (including the identification of LO7 and TO1 as macroscopic interface phonons) give rise to displacements in different directions. Other modes are not presented. Antisymmetric displacement patterns do not differ for $\theta = 0$ and $\theta = \pi/2$. Apart from the symmetry their behaviour is similar to that for symmetric

vibrations and $\theta = 0$. The s-polarised TOn modes exhibit completely the same displacement patterns in the x direction as the p-polarised modes for $\theta = 0$ and y polarisation.

The macroscopic and microscopic lineshapes as well as the directions of displacements in figure 1 agree essentially for $\theta = 0$, the case in which the long-range electric fields (2) and (5) are zero. The numbers of nodes are equal and both types of displacement vanish in the boundary regions. Small discrepancies concern the displacement amplitudes near the interfaces inside the GaAs material and the weak penetration of the lattice vibrations into the AlAs layers. In the $\theta = \pi/2$ case the same nearly perfect agreement is observed also for LO1, TO3, LO5, TO5 and TO7. The long-range electric fields $E_{jy}(\theta)$ and $D_{jz}(\theta)$ of the microscopic theory (2) almost vanish as in the continuum treatment. In the case of the other modes the situation is more complicated. The electric fields (5) which are only different from zero within the dispersionless continuum theory for the two interface modes LO7 and TO1 also accompany the microscopic vibration LO3 with respect to energy above LO7 and TO1. This phonon exhibits partial interface character due to the inclusion of the bulk phonon dispersion. In the microscopic approach, LO3 and TO1 change the polarisation directions going from $\theta = 0$ to $\theta = \pi/2$. From this point of view they should be classified as interface phonons. The displacement patterns indicate the same interface character. Despite the characterisation as interface phonon in the continuum approach, LO7 describes a confined mode within the microscopic treatment.

In summary, our strict comparison of lattice vibrational properties resulting within the continuum theory or a parallel microscopic model exhibits similarities but also limitations of the continuum approach neglecting bulk phonon dispersion. This remains valid even after utilisation of the uncertainties appearing in a dispersionless theory in an appropriate way and changing the solutions quoted usually in the conventional macroscopic approach. In more detail we state the following similarities and discrepancies

(i) The spectrum resulting within a dispersionless theory is quite different from that obtained on inclusion of the bulk phonon dispersion. Apart from the interface modes the only vibronic levels of the continuum model are given by $\omega_{\mathrm{LO}b}$ and $\omega_{\mathrm{TO}b}$.

(ii) For all modes which are not accompanied by long-range electric fields $E_{jy}(\theta)$ and $D_{jz}(\theta)$ the lineshapes of the displacement patterns resulting within the macroscopic continuum theory and a parallel microscopic model agree widely if appropriate solutions of the continuum approach are taken into account.

(iii) Small discrepancies between the two theories mainly concern the boundary regions. The envelope functions vanish at the interfaces whereas the confinement in the microscopic theory is not complete owing to the finite bulk phonon dispersion.

(iv) The comparison in the case of the p-polarised symmetrical LOn and TOn modes ($\theta > 0$) exhibits some problems due to the appearance of the long-range electric fields. In the dispersionless continuum theory these fields influence only the interface phonon branches. Owing to the inclusion of the bulk optical phonon dispersion in the microscopic description this field influence is more or less distributed among all p-polarised symmetrical phonons.

(v) The main failure of the continuum theory is due to the neglect of the bulk phonon dispersion. Boundary conditions of the macroscopic electrostatics can be further applied.

Acknowledgments

We thank M Cardona and R Enderlein for initiating this work. Fruitful discussions with A Fasolino, E Molinari and L Wendler are acknowledged.

References

[1] Sood A K, Menendenz J, Cardona M and Ploog K 1985 *Phys. Rev. Lett.* **54** 2111–4, 2115–8
[2] Jusserand B, Paquet D and Regreny A 1985 *Superlatt. Microstruct.* **1** 61–6
[3] Fasol G, Tanaka M, Sakaki H and Horikoshi Y 1988 *Phys. Rev.* B **38** 6056–65
[4] Wang Z P, Han H X, Li G H, Jiang D S and Ploog K 1988 *Phys. Rev.* B **38** 8483–5
[5] Pokatilov E P and Beril S I 1983 *Phys. Status Solidi* b **118** 567–73
[6] Babiker M 1986 *J. Phys. C: Solid State Phys.* **19** 683–97
[7] Enderlein R, Bechstedt F and Gerecke H 1988 *Phys. Status Solidi* b **148** 173–83
[8] Enderlein R 1988 *Phys. Status Solidi* b **150** 85–101
[9] Molinari E, Fasolino A and Kunc K 1986 *Superlatt. Microstruct.* **2** 397–400
[10] Richter E and Strauch D 1987 *Solid State Commun.* **64** 867–70
[11] Ren S-F, Chu H and Chang Y-C 1988 *Phys. Rev.* B **37** 8899–911, 10746–55
[12] Bechstedt F and Gerecke H 1989 *Phys. Status Solidi* b **154** 565–82
[13] Huang K and Zhu B-F 1988 *Phys. Rev.* B **38** 13377–85
[14] Bechstedt F and Gerecke H 1989 *Phys. Status Solidi* b **156** 151–170